International Journal of Physical Sciences

Academic Journals

ABOUT IJPS

The **International Journal of Physical Sciences (IJPS)** is published weekly (one volume per year) by Academic Journals.

International Journal of Physical Sciences (IJPS) is an open access journal that publishes high-quality solicited and unsolicited articles, in English, in all Physics and chemistry including artificial intelligence, neural processing, nuclear and particle physics, geophysics, physics in medicine and biology, plasma physics, semiconductor science and technology, wireless and optical communications, materials science, energy and fuels, environmental science and technology, combinatorial chemistry, natural products, molecular therapeutics, geochemistry, cement and concrete research, metallurgy, crystallography and computer-aided materials design. All articles published in IJPS are peer-reviewed.

Contact Us

International Journal of Physical Sciences

ARTICLES

Full Length Research Paper

Analysis of Hermite's equation governing the motion of damped pendulum with small displacement

Agarana M. C.* and Iyase S. A.

Department of Mathematics, Covenant University, Ota, Nigeria.

This paper investigates simple pendulum dynamics, putting damping into consideration. The investigation begins with Newton's second law of motion. The second order differential equation governing the motion of a damped simple pendulum is written in form of Hermite's differential equation and general solution obtained by means of power series. The results obtained are in agreement with the existing ones, and converge fast.

Key words: Pendulum, Hermite's equation, dynamics, damping, angular displacement.

INTRODUCTION

The pendulum is a dynamical system (Broer et al., 2010). The free pendulum consists of a rod, suspended at a fixed point in a vertical plane in which the pendulum can move (Agarana and Agboola, 2015; Nelson and Olsson, 1986). When a pendulum is acted on, both by a velocity dependent damping force, and a periodic driving force, it can display both ordered and chaotic behaviors, for certain ranges of parameters (Broer et al., 2010; Randall, 2003). The free, damped pendulum has damping, dissipation of energy takes place and a possible motion is bound to converge to rest (Peters 2002, 2003; Doumashkin et al., 2004; Gray, 2011). The motion of the bob of simple pendulum is a simple harmonic motion if it is given small displacement. When the pendulum is at rest, the only force acting on its weight and tension is the string. At the position, θ = 0°, the pendulum is in a stable equilibrium. Initial conditions are the way in which a system is started. The initial conditions for the simple pendulum are the starting angles, and the initial speed. In this paper we considered small angular displacement.

The equation governing damped simple pendulum can take the form of Hemite's differential equation (Moore, 2003). Our goal in this paper is to solve the resulting Hermite's equation from the equation governing the motion of a damped simple pendulum with small displacement by means of power series. The general solution of simple harmonic motion, generally, can be determined by means of power series.

Hermite's equation

Hermite's differential equation is (Moore, 2003)

$$\frac{d^2y}{dx^2} - 2x\frac{dy}{dx} + 2py = 0 \tag{1}$$

Where p is a parameter.

   The above second-order ordinary differential equation can be written as:

*Corresponding author. E-mail: michael.agarana@covenantuniversity.edu.ng

$$\frac{d^2y}{dx^2} - 2x\frac{dy}{dx} + \lambda y = 0 \tag{2}$$

Where $2p = \lambda$

This differential equation has an irregular singularity at ∞. It can be solved using the series method (Moore, 2003; Broer et al., 2010).

$$\frac{d^2y}{dx^2} - 2x\frac{dy}{dx} + \lambda y =$$
$$\sum_{n=0}^{\infty}(n+2)(n+1)a_{n+2}\,x^n + \sum_{n=0}^{\infty} -2na_n\,x^n + \qquad \sum_{n=0}^{\alpha} \lambda a_n\,x^n \tag{3}$$

$$\sum_{n=0}^{\infty}[(n+2)(n+1)a_{n+2} - 2na_n + \lambda a_n]x^n = 0 \tag{4}$$

The eventual linearly independent solutions can be written as (Moore, 2003)

$$y_1 = a_0\left[1 - \frac{\lambda}{2!}x^2 - \frac{(4-\lambda)\lambda}{4!}x^4 - \frac{(8-\lambda)(4-\lambda)\lambda}{6!}x^6 - \ldots\right] \tag{5}$$

$$y_2 = a_1\left[x + \frac{(2-\lambda)}{3!}x^3 + \frac{(6-\lambda)(2-\lambda)}{5!}x^5 + \ldots\right]. \tag{6}$$

Theorem

If the function P(x) and Q(x) can be represented by power series

$$P(x) = \sum_{n=0}^{\infty} P_n(x - x_0)^n \tag{7}$$

$$Q(x) = \sum_{n=0}^{\infty} q_n(x - x_0)^n \tag{8}$$

with positive radii of convergence R_1 and R_2 respectively, then any solution y(x) to the linear differential equation

$$\frac{d^2y}{dx} + P(x)\frac{dy}{dx} + Q(x)y = 0 \tag{9}$$

can be represented by a power series

$$y(x) = \sum_{n=0}^{\infty} a_n(x - x_0)^n \tag{10}$$

whose radius of convergence is less than or equal to the smaller of R_1 and R_2.

GOVERNING EQUATIONS AND SOLUTION PROCEDURES

The equation of motion for damped, driven pendulum of mass m and length l can be written as (Agarana and Agboola, 2015):

$$ml^2\frac{d^2\theta}{dt^2} + \gamma\frac{d\theta}{dt} + mgl\sin\theta = C\cos(w_D t) \tag{11}$$

Where the right hand side of Equation (1) is the driving force.

Suppose the damped pendulum is not driven, then the right hand side of Equation (1) is zero, and Equation (11) becomes:

$$ml^2\frac{d^2\theta}{dt^2} + \gamma\frac{d\theta}{dt} + mgl\sin\theta = 0 \tag{12}$$

The three terms on the left hand side of Equation (12) are the acceleration, damping and gravitation respectively. θ is the angular displacement, t is the time, l is the length, m is the mass, γ is the dissipation coefficient and g is the acceleration due to gravity. Dividing Equation (12) by ml^2 we have

$$\frac{d^2\theta}{dt^2} + \frac{\gamma}{ml^2}\frac{d\theta}{dt} + \frac{g}{l}\sin\theta = 0 \tag{13}$$

For a small angular Displacement, $\theta \approx \sin\theta$. Therefore Equation (13) becomes:

$$\frac{d^2\theta}{dt^2} + \frac{\gamma}{ml^2}\frac{d\theta}{dt} + \frac{g}{l}\theta = 0 \tag{14}$$

At this stage, we carefully choose the values of t and p such that:

$$\frac{\gamma}{ml^2} = -2t \text{ and } \frac{g}{l} = 2p \tag{15}$$

Where p is a parameter.

Substituting Equation (15) into Equation (14) we have:

$$\frac{d^2\theta}{dt^2} - 2t\frac{d\theta}{dt} + 2p\theta = 0 \tag{16}$$

Equation (16) is Hermite's differential equation. Indeed

P(t) = -2t, and Q(t) = 2p

Both functions being polynomials, have power series about $t_o = 0$ with infinite radius of convergence (Moore, 2003). The angular displacement θ is a function of t and satisfies simple harmonic motion characteristics. Any solution θ(t) to Equation (16) can be represented by a power series (Agarana and Agboola, 2015; Moore, 2003):

$$\theta(t) = \sum_{n=0}^{\infty} a_n(t - t_0)^n \tag{17}$$

$$\therefore \theta(t) = \sum_{n=0}^{\infty} a_n t^n, \quad since \ (t_0 = 0) \tag{18}$$

Differentiating term by term we have

$$\frac{d\theta}{dt} = \sum_{n=1}^{\infty} na_n t^{n-1} \tag{19}$$

$$\frac{d^2\theta}{dt^2} = \sum_{n=2}^{\infty} n(n-1)a_n t^{n-2} \tag{20}$$

Replacing n by $m+2$ in Equation (10), we have

$$\frac{d^2\theta}{dt^2} = \sum_{m+2-2}^{\infty}(m+2)(m+2-1)a_{m+2} t^{m+2-2} \tag{21}$$

$$= \sum_{m=0}^{\infty}(m+2)(m+1)a_{m+2} t^m \tag{22}$$

And then replacing m by n once again, so that

$$\frac{d^2\theta}{dt^2} = \sum_{n=0}^{\infty}(n+2)(n+1)a_{n+2}\, t^n \tag{23}$$

From Equation (19)

$$-2t\frac{d\theta}{dt} = \sum_{n=0}^{\infty}-2na_n\, t^n \tag{24}$$

Also from Equation (18)

$$2p\theta = \sum_{n=0}^{\infty} 2pa_n\, t^n \tag{25}$$

Adding together Equations (23), (24) and (25), we have

$$\frac{d^2\theta}{dt^2} - 2t\frac{d\theta}{dt} + 2p\theta = \sum_{n=0}^{\infty}(n+2)(n+1)a_{n+2}\, t^n + \sum_{n=0}^{\infty}-2na_n\, t^n + \sum_{n=0}^{\alpha} 2pa_n\, t^n \tag{26}$$

$$= \sum_{n=0}^{\infty}(n+2)(n+1)a_{n+2}\, t^n + \sum(-2n+2p)a_n\, t^n \tag{27}$$

Since θ satisfies Hermite's equation, we have

$$0 = \sum_{n=0}^{\infty}[(n+2)(n+1)a_{n+2} + (-2n+2p)a_n\,]t^n \tag{28}$$

$$\Rightarrow (n+2)(n+1)a_{n+2} + (-2n+2p)a_n = 0 \tag{29}$$

$$\Rightarrow a_{n+2} = \frac{2n-2p}{(n+2)(n+1)}\, a_n \tag{30}$$

In order to determine the values of a_0, a_1, a_2, a_3...in the above power series, the first two coefficients, a_0 and a_1 can be determined from the initial conditions as (Moore, 2003):

$$\theta(0) = a_0 \; and \; \frac{d\theta}{dt}(0) = a_1 \tag{31}$$

While the other coefficients are determined by equating n to 0, 1, 2, 3, ... to obtain, from Equation (30), as (Moore, 2003):

$$a_2 = \frac{2P}{2.1}\, a_0 \tag{32}$$

$$a_3 = -\frac{2(P-1)}{3!}\, a_1 \tag{33}$$

$$a_4 = \frac{2^2P(P-2)}{4!}\, a_0 \tag{34}$$

$$a_5 = \frac{2^2(P-1)(P-3)}{5!}\, a_1 \tag{35}$$

$$a_6 = \frac{-2^3P(P-2)(P-4)}{6!}\, a_0 \tag{36}$$

and so forth.
Equation (28) can now be written as follows:

$$\theta = a_0\left[1 - \frac{2P}{2!}t^2 + \frac{2^2P(P-2)}{4!}t^4 - \frac{2^3P(P-2)(P-4)}{6!}t^6 + \cdots\right] + a_1\left[t - \frac{2(P-1)}{3!}t^3 + \frac{2^2(P-1)(P-3)}{5!}t^5 - \frac{2^3(P-1)(P-3)(P-5)}{7!}t^7 + \cdots\right] \tag{37}$$

We now write the general solution to Equation (16) in the form

$$\theta = a_0\theta_0(t) + a_1\theta_1(t) \tag{38}$$

where

$$\theta_0(t) = 1 - \frac{2P}{2!}t^2 + \frac{2^2P(P-2)}{4!}t^4 - \frac{2^3P(P-2)(P-4)}{6!}t^6 + \cdots \tag{39}$$

and

$$\theta_1(t) = t - \frac{2(P-1)}{3!}t^3 + \frac{2^2P(P-1)(P-3)}{5!}t^5 - \frac{2^3(P-1)(P-3)(P-5)}{7!}t^7 + \cdots \tag{40}$$

$\theta_0(t)$ and $\theta_1(t)$ form a basis for the space of solutions to Equation (16) which is hermite's equation (Moore, 2003).
For different values of the parameter p, we obtain different values of θ. When p is a positive integer, one of the two power series will collapse, yielding a polynomial solution known as Hermite Polynomial (Moore, 2003). The initial conditions which we are choosing for the purpose of this paper are:

$$\theta(t = 0) = a_0 \; ; \; \frac{d\theta}{dt}(t = 0) = a_1 = 0$$

Where a_0 is a constant whose value we will take as input.
From these initial conditions, $a_1 = 0$ and a_0 is a constant. Therefore Equation (38) becomes

$$\theta = a_0\theta_0(t) + 0 \tag{41}$$

That is,

$$\theta = a_0\left[1 - \frac{2P}{2!}t^2 + \frac{2^2P(P-2)}{4!}t^4 - \frac{2^3P(P-2)(P-4)}{6!}t^6 + \cdots\right] \tag{42}$$

For different values of parameter p and a particularly value of constant a_0, we can see the angular displacement θ at the different time (t). Recall from Equation (15) that

$$p = \frac{g}{2l} \; and \; t = \frac{-\gamma}{2ml^2}$$

$$\therefore \theta = a_0\left[1 - \frac{g/l}{2!}\left(\frac{-\gamma}{2ml^2}\right)^2 + \frac{2g/l\left(\frac{g}{2l}-2\right)\left(\frac{-\gamma}{2ml^2}\right)^4}{4!} - 2^3\left(\frac{g}{2l}\right)\left(\frac{g}{2l}-2\right)\left(\frac{g}{2l}-4\right)\left(\frac{-\gamma}{2ml^2}\right)^6 + \cdots\right] \tag{43}$$

Also Equation (42) can be written by substituting $\frac{g}{2l}$ for p as follows:

$$\theta = a_0\left[1 - \frac{g}{2l}t^2 + \frac{1}{6}\left(\frac{g}{2l}\right)\left\{\frac{g}{2l}-2\right\}t^4 - \frac{1}{90}\left(\frac{g}{2l}\right)\left(\frac{g}{2l}-2\right)\left(\frac{g}{2l}-4\right)t^6 + \cdots\right] \tag{44}$$

The general solution as given in Equation (38) implies that

$$\theta = 1 - \frac{2P}{2!}t^2 + \frac{2^2P(P-2)}{4!}t^4 - \frac{2^3P(P-2)(P-4)}{6!}t^6 + \cdots + t - \frac{2(P-1)}{3!}t^3 + \frac{2^2P(P-1)(P-3)}{5!}t^5 - \frac{2^3(P-1)(P-3)(P-5)}{7!}t^7 + \cdots \tag{45}$$

It is assumed that $a_0 = 1$ and $a_1 = 1$.

$$\theta = 1 + t - \frac{2P}{2!}t^2 - \frac{2(P-1)}{3!}t^3 + \frac{2^2P(P-2)}{4!}t^4 + \frac{2^2P(P-1)(P-3)}{5!}t^5 - \frac{2^3P(P-2)(P-4)}{6!}t^6 - \frac{2^3(P-1)(P-3)(P-5)}{7!}t^7 + \cdots$$

$$\therefore \tag{46}$$

TIME PERIOD AND DISSIPATION COEFFICIENT EFFECTS ON THE ANGULAR DISPLACEMENT

Time period of oscillation for small displacement

The time period of oscillation of a simple pendulum with a small displacement is given as (Agarana and Agboola, 2015; Davidson, 1983)

$$T = 2\pi \sqrt{\frac{l}{g}} \tag{47}$$

Where l is the length of the pendulum and g is the acceleration due to gravity, respectively.
Equation (50) can the written as:

$$T = \pi \sqrt{\frac{2}{p}} \tag{48}$$

Both Equations (47) and (48) show that the period T is a function of the length of the pendulum, just as equation (48) the angular displacement is a function of the length of the pendulum (since $p = \frac{g}{2l}$) and time. The time period of oscillation, for small displacement, as it affects the motion of the pendulum is determined by the length of the pendulum.

Effect of the dissipation coefficient γ

From Equation (15),

$$\gamma = -2tml^2 \tag{49}$$

Also $l = \frac{g}{2P} \tag{50}$

Substituting Equation (50) into Equation (40), we have

$$\gamma = -2tm \left(\frac{g}{2P}\right)^2 \tag{51}$$

$$\gamma = -\frac{ml}{2}\left(\frac{g}{2P}\right)^2 , \; (l \text{ taken to be } 4t) \tag{52}$$

At different values of m and particular value of l, we can see how γ behaves.

NUMERICAL RESULTS AND DISCUSSION

We illustrated the ideas presented in the previous sections by means of a more realistic numerical example. As an illustration, therefore, the following values were adopted: l = 10, 20, 30, 40; $a_0 = 1, 2, 3, 4$, 5 and $g = 9.81$. We therefore determined the values of the angular displacement (θ) for different lengths (l) of the pendulum and at different initial values of the angular displacement (a_0). From Figure 1, we can see that when the length of the pendulum is 10, the value of the angular displacement (θ) increases as its initial value (a_0) increases. This happens at the initial time, up to time t=0.8 where there is a convergence of the different values of θ at different values of a_0. However after time t=0.8 the opposite became the case: as initial angular displacement increases the angular displacement decreases. The same explanation goes for the dynamic behaviour of the pendulum as shown in Figures 2, 3 and 4, but the value of the angular displacement start decreasing as the value of a_0 increases at different times. For instance, in Figure 2, it starts at time t = 0.9, in Figure 3, it starts at time t = 0.95, and in Figure 4, it starts at time t = 1. We therefore observe, generally, that as we increase the value of the initial angular displacement, the subsequent angular displacement increases initially and decreases after some time, depending on the length l of the pendulum. The higher the value of l, the longer it takes for the change in the motion pattern of the pendulum as regards its angular displacement.

For various values of the pendulum length (l), the angular displacement of the pendulum for various values of the initial angular displacement a_0 (that is, a_0=1, a_0=2, a_0=3, a_0=4, a_0=5) considered were calculated and are plotted in Figures 5, 6, 7 and 8 as functions of time. Specifically in Figure 5, the angular displacement profile of the damped pendulum is depicted for a_0 =1 and with the pendulum length (l), as a parameter. The corresponding curves for a_0=2, 3 and 4 are shown in Figures 6, 7, and 8 respectively. Clearly, from the figures the angular displacement increases with an increase in the value of the initial angular displacement for fixed values of pendulum length. Also for specific value of the initial angular displacement, the subsequent angular displacement increases as the pendulum length increases. However, the angular displacement decreases with time irrespective of the values of the pendulum length and the initial angular displacement. In Figures 9 and 10, the angular displacement of the damped pendulum for different values of pendulum length (l) and the period (T) respectively, with non-zero value of the angular velocity (a_1), is plotted as a function of time. Evidently, it can be noticed in Figure 9 that the angular displacement increases with time and as the pendulum length increases. Also in Figure 10, angular displacement increases with time and as the pendulum period increases. The similarity in Figures 9 and 10 is as a result of the fact that the period (T) is a function of the length of the pendulum (l). Considering the effects of damping and mass of the pendulum bob on the angular displacement of the damped pendulum; angular pendulum for various values of the damping factor and mass of the pendulum bob were calculated and plotted in Figures 11 and 12
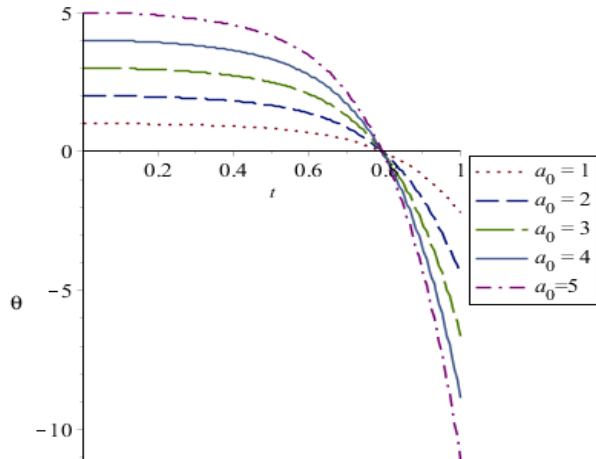
Figure 1. Angular displacement of pendulum at l = 10, a_1 = 0 and different values of a_0 and time.
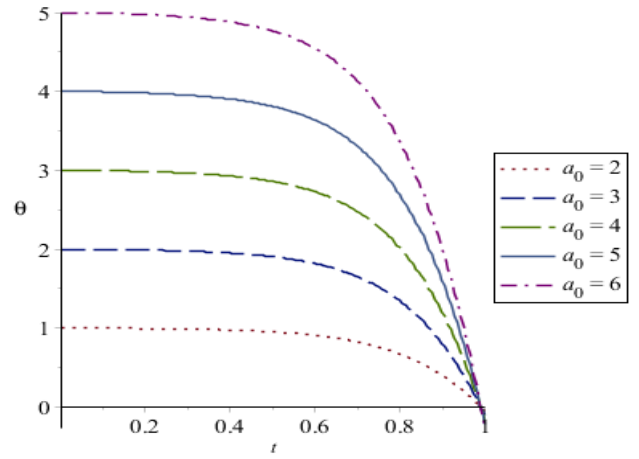
Figure 4. Angular displacement of pendulum at l = 40, a_1 = 0 and different values of a_0 and time.
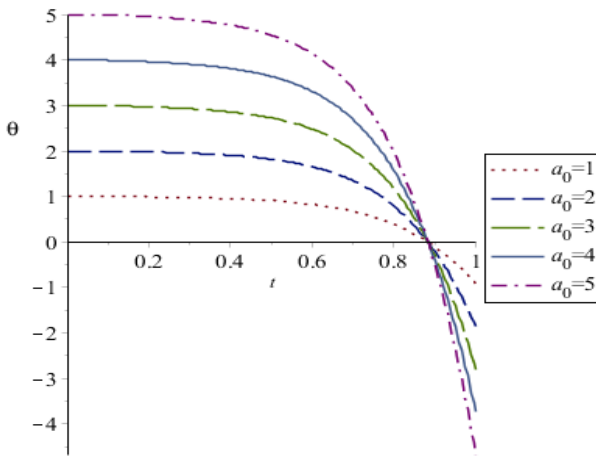
Figure 2. Angular displacement of pendulum at l = 20, a_1 = 0 and different values of a_0 and time.
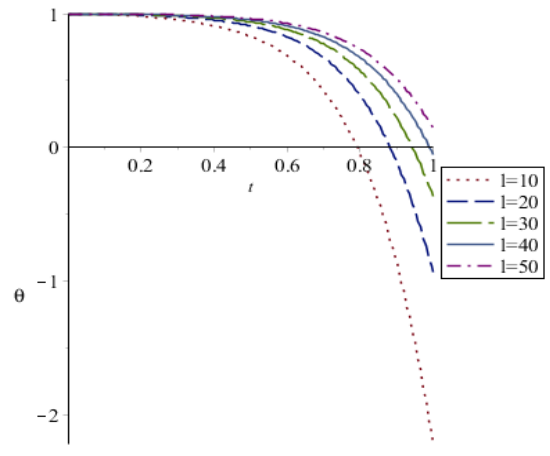
Figure 5. Angular displacement of pendulum at a_0 = 1 and different lengths and time.
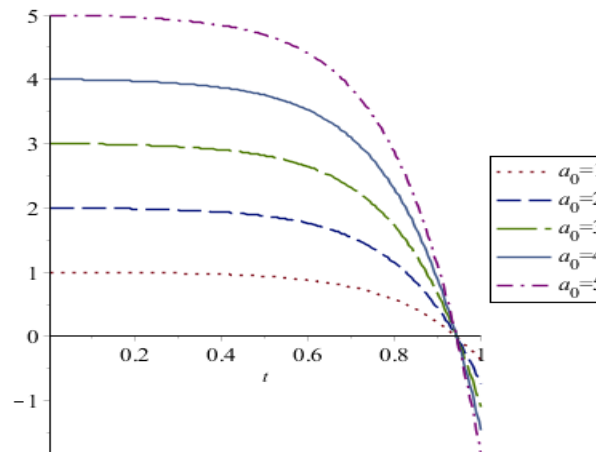
Figure 3. Angular displacement of pendulum at l = 30, a_1 = 0 and different values of a_0 and time.
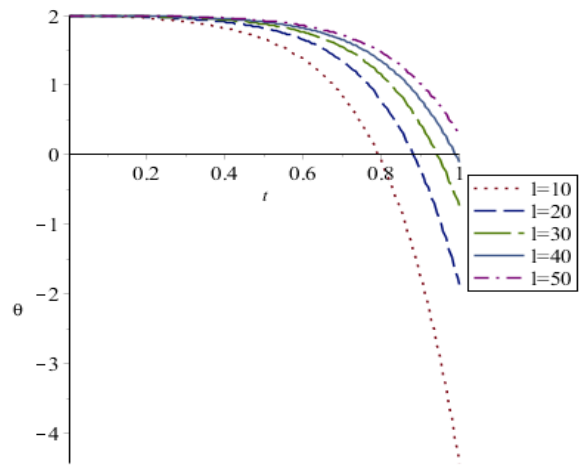
Figure 6. Angular displacement of pendulum at a_0 = 2 and different lengths and time.
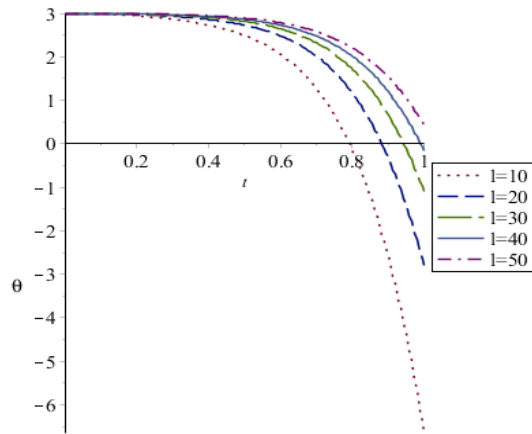
Figure 7. Angular displacement of pendulum at $a_0 = 3$ and different lengths and time.
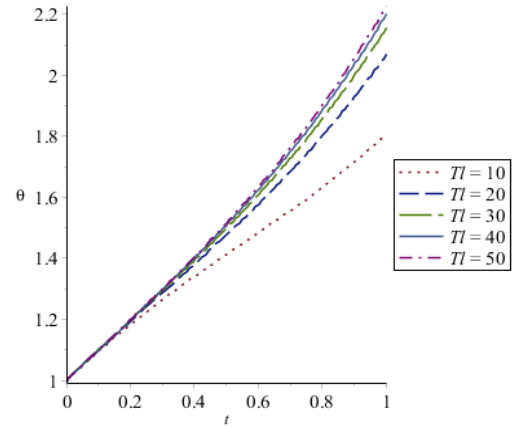
Figure 8. Angular displacement of pendulum at $a_0 = 4$ and different lengths and time.

Figure 9. Angular displacement of pendulum with non-zero initial angular velocity and different values of initial angular displacement, time and lengths.

Figure 10. Angular displacement of pendulum with non-zero initial angular velocity and different values of initial angular displacement, time and period.

Figure 11. Effect of the damping factor on angular displacement of the pendulum.
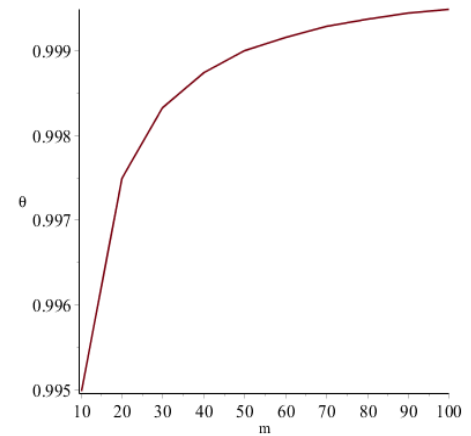
Figure 12. Effect of the mass on angular displacement of the pendulum.
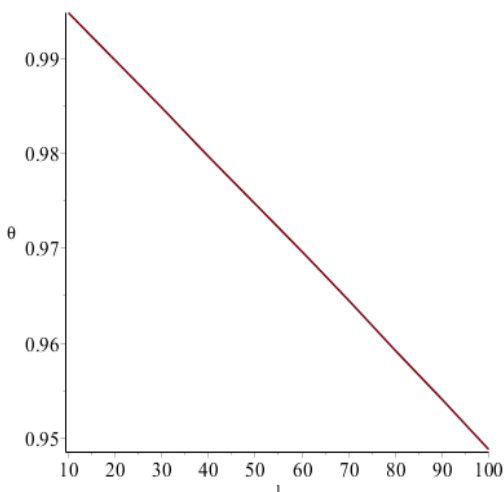
Figure 13. Effect of the length of pendulum on the angular displacement.

respectively. It can be seen from Figure 11 that the angular displacement increases sharply initially with an increase in the damping, then subsequently drops until becoming almost asymptotic to straight line $\theta = 1,$ parallel to the horizontal axis. Similarly, in Figure 12 the angular displacement initially increases sharply as the mass of the pendulum bob increases, then gradually drops until becoming almost asymptotic to the straight line $\theta = 1,$ parallel to the horizontal axis. From the two figures it implies that both the damping factor and mass of the pendulum bob have impact on the angular displacement of the pendulum. As we can see, as these parameters increase the angular displacement increases. Figure 13 shows clearly that apart from the fact that an increase in pendulum length will increase. The relationship between the angular displacement and length of the pendulum can be considered to be directly proportional and positively correlated.

CONCLUSION

The angular displacement of a damped pendulum with small displacement is analysed on the basis of Hermite's form of governing equation of a damped simple pendulum. The general solution of the equation of motion governing damped simple pendulum, put in Hermite equation form, was obtained by means of power series. Analysis reveals that for different values of the initial angular displacement, we get different values of the subsequent angular displacement. There is a direct correlation. Also, it is revealed that the length of the pendulum affects the angular displacement; the length of

the pendulum is directly proportional to the angular displacement of the pendulum. We notice that the effect of the period of the pendulum is similar to that of the length of the pendulum. This is because the period of the pendulum is a function of the length of the pendulum. Both th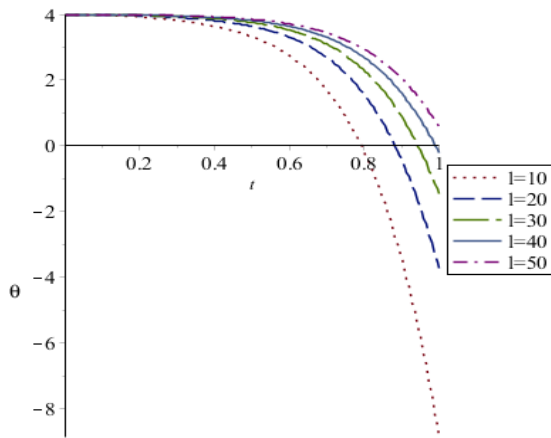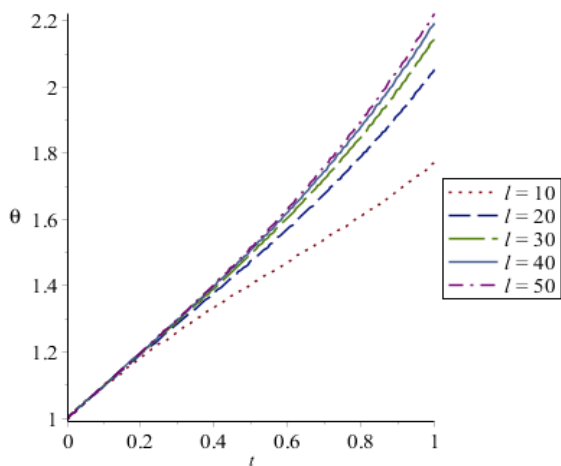e damping and the mass of the bob also have effect on the angular displacement of the pendulum in almost the same manner.

Conflict of Interest

The authors have not declared any conflict of interest.

ACKNOWLEDGEMENT

REFERENCES

Agarana MC, Agboola OO (2015). Dynamic analysis of damped driven pendulum using laplace transform method. Int. J. Math. Comput. 26:3.
Doumashkin P, Litster D, Prtiched D, Surrow B (2004). Pendulums and collisions, Mitopencourseware, Massachusetts Institute of Technology.
Davidson GD (1983). The damped Driven Pendulum: Bifurcation analysis of experimental data, a thesis presented to the division of mathematics and natural sciences, Reed Collzz   Feigenbaum, M.J., Universal behavior in nonlinear systems. Physica D: Nonlinear Phenomena. 7(1-3):16-39.
Gray DD (2011). The damped driven pendulum: Bifurcation analysis of experimental data. A Thesis for the Division of Mathematics and National Sciences, Read College.
Moore JD (2003). Introduction to partial differential equations. P. 10. http://www.math.ucsb.edu/~moore/pde.pdf
Nelson RA, Olsson MG (1986). The pendulum--rich physics from a simple system. Am. J. Phys. 54:2.
Broer HW, Hasselblatt B, Takens F (Eds) (2010). Handbook of Dynamical Systems. Vol. 3, North-Holland, 2010.
Peters R (2002). "The pendulum in the 21st century--relic or trendsetter", proc. Int'l pendulum conf., Sydney. Online at http://arXiv.org/html/physics/0207001/
Peters R (2003). Model of internal friction damping in solids". http://arxiv.org/html/physics/0210121
Randall DP (2003). Nonlinear Damping of the Linear Pendulum, Mercer University   Macon,   Georgia,   Accessed   2003: arxiv.org/pdt/physics/0306081

Full Length Research Paper

Particle production in proton-proton collisions

M. T. Ghoneim[1], F. H. Sawy[2] and M. T. Hussein[1]

[1]Department of Physics, Faculty of Science, Cairo University, Giza, Egypt.
[2]High Energy Physics (HEP) lab, Physics Department, Faculty of Science, Cairo University, Giza, Egypt.

Proton-proton collision is a simple system to investigate nuclear matter and it is considered to be a guide for more sophisticated processes in the proton-nucleus and the nucleus-nucleus collisions. In this article, the authors present a phenomological study of how the mechanism of particle production in pp interaction changes over a wide range of interaction energy. This study is done on data of charged particle produced in pp experiments at different values of energy. Some of these data give the created particles classified as hadrons, baryons and mesons, which help us compare between production of different particles. This might probe some changes in the state of nuclear matter and identify the mechanism of interaction.

Key words: String, gluon fragmentation, jet production.

INTRODUCTION

The concept of mass-energy relationship of particle production has always been one of the selected topics to investigate in high energy nuclear reactions over several decades. This type of research has probably started by the time people wanted to accelerate particles up to relativistic speeds and to smash them into other particles and see what may turn out. Passing over the techniques of acceleration and particle detection, people observed that in proton-proton (pp) collisions at relativistic energy, more particles came out than those that went in. The extra particles that came out were principally created pions and/or heavier particles at higher interaction energies. The authors main task in this work is to follow up, qualitatively, the variation of the average multiplicity and distribution of created particles with the reaction energy by making use of the available experimental data and their corresponding theoretical aspects over a wide range of interaction energy; from few GeV up to several TeV.

Particle creation between theory and experiment

The physical nature of proton-proton interactions varies with energy as a result of the decrease of the coupling constant with energy. This fact could lie behind the inability to find a unique theory to describe particle creation mechanism in p-p interactions over the whole available energy range. Such creation goes through phenomenological models in low energy region to perturbative quantum chromo-dynamics (PQCD) in high energy one (Daniel et al., 2003; Adler et al., 2003; Regge, 1959; Gribov, 1967).

In view of one of the most useful models in this subject;
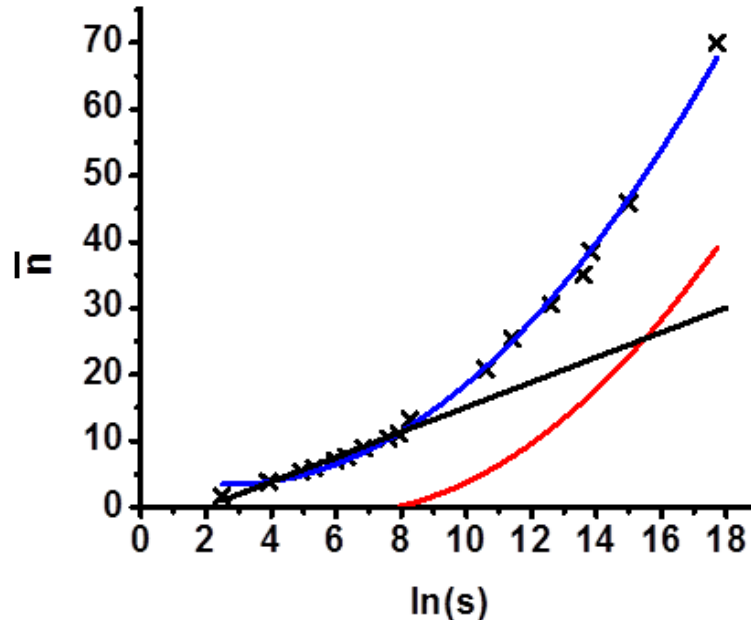
Figure 1. The mean multiplicity of created particles, $\bar{n}$, as a function of ln(s). Crosses are experimental data; straight line is the fitting with the low energy part of the data; the blue curve is the fitting with whole data and the red curve represents the semi-hard and the hard classes of the events, respectively.

the "String Model", two protons, each containing three valence quarks, interact by color field exchange which resembles a string. The collision energy divides each proton into its constituent quarks to form strings between the quarks (diquarks) from the projectile and the target. The string forces between the color charges cause periodical oscillations of the system and the color field may materialize at a point of the string. As time develops, the string breaks randomly into smaller pieces carrying smaller fraction of the initial energy. The primary string is formed among the originally interacting quarks while a secondary string is generated in the field of sea quarks of the primary string and so on for higher order strings. Assuming z to be a fraction of energy carried by a string, it continues producing particles in a ranking order governed by a fragmentation function, $f(z)$, until the residual energy becomes less than the threshold of production. Some string dynamics (Hussein et al., 1995) that consider higher orders, assume that a jet is formed by an original quark q_0, initially with energy w_0, where at the first vertex of fragmentation, the string breaks forming a $q\bar{q}$ with energy zw_0 leaving the string with energy $w_1=(1-z)w_0$, where $0<z<1$ with the distribution $f(z)$. Further fragmentation of the string would produce $q\bar{q}$ pairs forming particles whose i^{th} rank order having energy zw_{i-1}. The length of the string would depend upon the quark energy w_0 and $f(z)$. One would expect that the longer the string, the larger the number of vertices and the higher the multiplicity of the formed mesons. If z_{av} is the average value of the parameter z, then the residual energy of the string after the nth rank would be:

$$w_n = (1 - z_{av})^{\bar{n}} w_0 \tag{1}$$

where

$$\bar{n} = \ln(w_0/w_n)\beta \tag{2}$$

With:

$$\beta = -1/\ln(1 - z_{av}) \tag{3}$$

$\bar{n}$, is the average multiplicity of the produced particles. When the mass of a string piece gets small enough, it is identified as a hadron and the breaking stops within that piece meaning that the whole system eventually evolves into hadrons (hadronization process). Figure 1 presents the dependence of the average multiplicity on the the center of mass energy, s, over the whole range of data. Crosses in this figure are experimental data (Badawy, 2008; Minami, 1973; http.//pdg.lbl.gov, Biyajima et al., 2001; Wolschin, 2011) while the blue curve is their polynomial fit:

$$\bar{n} = a\,(\ln s)^2 + b\ln s + c \tag{4}$$

The values of the fitting parameters; a, b and c are: 0.29, -1.57 and 5.61.

One may start with the "softly" created particles, where the average multiplicity, in the lower energy portion of Figure 1, shows a linear logarithmic relationship with the energy the fit of which is given by the straight line with fitting parameters 0, 1.0 and -3.66 in Equation 4, respectively. This linearity, that does not describe the data in the higher energy region (as its extension shows) is supported by the Fermi scaling, as well as by most of theoretical models like the "multi-peripheral model" and the "quark-parton model" in asymptotic soft regions (Cerny and Pisut, 1977; Fiete et al., 2010). The parameterization works reasonably and this linearity fits well up to several tens of GeV. The multiplicity distribution of created particles by soft events follows a Poisson distribution:

$$P(n) = \frac{\bar{n}^n}{n!} e^{-\bar{n}} \tag{5}$$

which means that every single final-state particle is created and emitted independently and viewed as a black body radiation (Niccol`o, 1998). The KNO scaling of the multiplicity distribution (within this energy range) for non-single diffractive NSD events in full phase space supports a single creation mechanism (Koba et al., 1972).

Above the last stated energy range, the multiplicity distribution shows a deviation from the Poisson shape, predicting some kind of correlations between the created particles and a sign of variation in the creation mechanism. These correlations were proposed by the "Clan Model" (Fiete et al., 2010), that assumes the ability of a particle to emit additional particles, as cascading by decay and fragmentation. The model considers that the created particles stream as clans (clusters) where the ancestors production, and thus the clans are governed by a Poisson distribution. A clan contains all particles that stem from the same ancestor, where the ancestors themselves are produced independently. The interpretation of "Clan Model" was based on the success of the Negative Binomial Distribution NBD of the particle multiplicity:

$$P(n; \bar{n}; k) = \binom{n+k-1}{n} \left(\frac{\bar{n}/k}{1+\bar{n}/k}\right)^n \frac{1}{(1+\bar{n}/k)^k} \tag{6}$$

which describes the multiplicity distributions up to $\sqrt{s} = 540$ GeV, announced by UA5 (Giovannini and Van-Hove, 1986). The NBD is defined by two parameters $\bar{n}$ and k. $\bar{n}$ is the average multiplicity as mentioned above and the parameter k is related to the dispersion D as:

$$\frac{D^2}{(\bar{n})^2} = \frac{1}{\bar{n}} + \frac{1}{k} \tag{7}$$

For $(1/k) \rightarrow 0$, the NBD reduces to the Poisson distribution, and for k = 1 it is the geometric distribution. It was found that $(1/k)$ increases almost linearly with $\ln(s)$ whereas KNO scaling corresponds to a constant, energy-independent.

The same meaning could be found in the string model that proposed multi-order fragmentation for higher energy. The interpretation had got more support by assuming new type of events, called "semi-hard" in addition to "soft" ones to produce these bundles. Experimentally, semi-hard events are responsible for a "mini-jet" production (Niccol`o, 1998). A "mini-jet" is defined as a group of particles having a total transverse momentum larger than 5 GeV/c (Tran and Van, 1988; Giovannini and Ugoccioni, 1999). As energy goes higher than 540 GeV; "semi-hard" events start to show significant contribution in collision and many models were modified by adding new terms. The Dual Parton Model (DPM) claims that "mini-jets" are generated from at least four chains, two of them come from a contribution of valence quarks and the other two are generated from sea quarks through semi-hard interaction. As energy goes higher, sea quark contribution goes bigger. Since sea quarks carry only a small fraction of the momentum of the incident hadrons, the chains are concentrated in the central rapidity region. Thus, these may explain the rise of the central particle density.

Consequently, the KNO scaling has been violated in this region. This violation is traced to short range correlations of particles in the strings and interplay between the double-pomeron processes (Niccol`o, 1998; Giovannini and Ugoccioni, 1999). The superposition of the two types of interaction affects the multiplicity distribution and therefore potentially explains the deviation from the scaling found at lower energies. UA5 has been successfully fitted the multiplicity distributions of created particles as a superposition of two independent NBDs, at $\sqrt{s} = 900$ GeV up to 1800 GeV, and this is supported by a two-component model (Niccol`o, 1998; Giovannini and Ugoccioni, 1999). The quadratic term was then found to be a better description of the data as the interaction energy goes above the limits of pure soft events stated before. This term reflects the contribution of semi-hard and gluon-bremsstrahlung process, that starts to manifest itself as the interaction energy gets into the TeV region (Giovannini and Ugoccioni, 1999). These radiation are known as Initial and Final State Radiations that emit gluon before and after real collision has occurred, respectively. These radiation (gluon) can materialize to produce hadrons and the increase in collision energy, increases the contribution of this radiation in particle production.

As energy goes higher, the strong coupling constant becomes smaller and smaller, slipping into asymptotic freedom. Collisions of pp at this higher energy can be viewed as quark-quark collisions which can be mathematically described by perturbative quantum
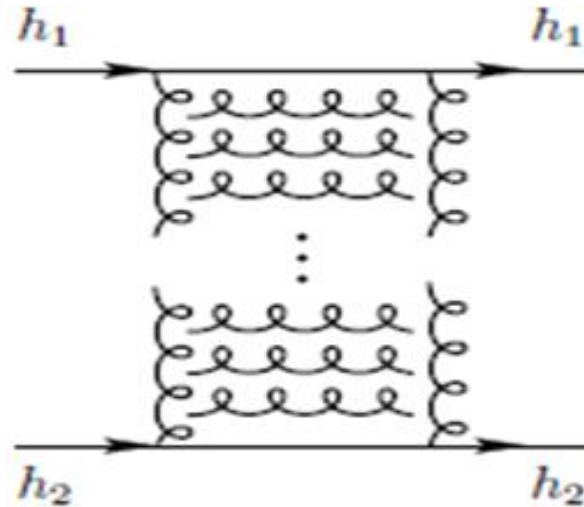
Figure 2. Multi-pomeron exchange diagram.

chromo-dynamics (PQCD). These high energy quark collisions generate new type of events called "hard" events in addition to "soft" and "semi-hard" ones. Hard quark interactions develop via short-distance over a very short time scale and the subsequent fragmentation produces a cone of hadronic final states that originate from the same quarks. This cone of hadrons is called a "jet", representing an independent fireball for hadron creation, and the properties of the jet depend only on the initial quark. The proposal of DPM is forming more than four chains by multiple pomeron exchanges (Figure 2), and increase the height of the central plateau with energy.

Therefore, the multi-chain contribution becomes increasingly important and the average number of chains increases with energy. The growth of multiplicity at higher energy can be understood by assuming that; as the interaction energy goes higher; gluon jets grow with higher multiplicity than the quark jets and both compete with each other to, eventually, produce particles through their multifragmentations. QCD predicts that gluon initiates jets to have higher average particle multiplicity compared to quark initiated ones (CMC collaboration, 2012). This is supported fairly by the red curve (Figure 2), that results from the subtraction of the staright line (which represents the softly produced multiplicity) from the total curve, to obtain the multiplicity relation that belongs to the semi-hard and hard mechanism events. One might add, at this point, that production of particles in the nuclear reaction is one of the macroscopic parameters to probe what is going on inside the reacting systems during the reaction and the development of the processes that take place in these systems as the interaction energy goes higher. The red cuve in Figure 1 indicates some phase change of the nuclear matter and consequently of the mechanism by which different types of particles are

created. This curve also shows the limit ($\sqrt{s}$ = 53 GeV) at which such a change started to occur. Some workers (STAR Collaboration, 2014a, b) has defined the hard event as that having at least one jet cluster while the soft one as that having no clusters at all; they also add that the relation between $< P_T >$ and the multiplicity in soft events has a weak dependence of the collision energy from the RHIC to the Tevatron and the properties of the final states are determined only by the number of the charged particles, while hard events have much stronger dependence. A recent study has described the multiplicity – energy relationship by a linear, quadratic and cubic terms in a polynomial. This study interpreted the second and third orders in their fitting polynomial as coming from double and triple quark interactions, respectively, rather than from only one (Ashwini et al., 2013; Alexopoulos et al., 1998; Walker, 2004).

In this research, so far, the authors have considered creation of particles without distinguishing between their entities. Let us shed some light on different types of created particles taken separately from different experimental data that have reasonable statistics and rational consistency (Antinucci et al., 1973; Rushbrooke, 1982; Samset, 2006; Engel, 2008; Ansorge et al., 1989; Anticic et al., 2010; Becattini and Heinz, 1997). The dependence of the mean multiplicity of created pions, keons and lambdas, $\bar{n}_{\pi}$, $\bar{n}_{k}$, $\bar{n}_{\Lambda}$; respectively, on ln(s), is displayed in Figure 3 and seems to follow a similar polynomial in Equation (4) with fitting paprameters given in Table 1. Figure 3 shows that below certain values of energy, the data do not show any production of pions, keons and lambdas and each type of these particles starts to appear as energy goes higher past certain values. This is easily understood if one takes into account the threshold of production of each type of these
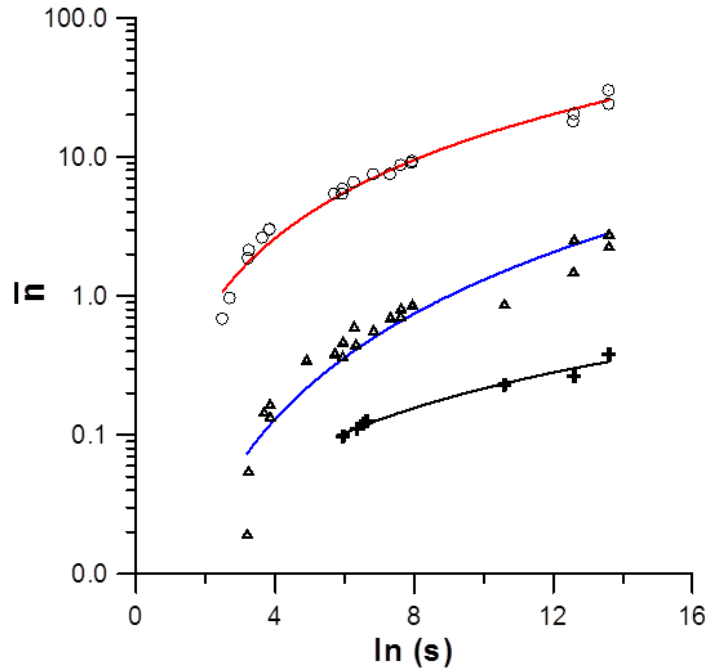
Figure 3. The mean multiplicities of created pions, $\bar{n}_\pi$, keons, $\bar{n}_k$ and lambdas $\bar{n}_\Lambda$ (circles, triangles and crosseses; respectively) as a function of ln(s) and the red, blue and black lines are their fittings, respectively.

Table 1. Fitting paprameters of Equation (4), with the experimental data of the created particles, namely, pions, keons and lambdas.

Created particle	Fitting parameters			
	a	b	c	d
Pions (red curve)	0.02	-0.35	3.42	-6.18
Keons (blue curve)	0	-0.09	0.72	-1.53
Lambdas (black line)	0	0	-0.03	0.17

particles. One may notice also that allover the considered energy range, production of pions is more dominant than keons and lambdas. This comes from the fact that creation of pions is more probable than creation of heavier particles, that is, the probability of u and d quarks is higher than s, which are responsible for the formation of heavier particles, in spite of the presence of energy that covers the thresholds of their creation. This fact, in turn, is probably a consequence of the color field nature that loses its energy bit by bit as excitations (kinks) of soft gluons rather than by hard single gluon radiation (Niccol`o, 1998; Tai and Sa, 1998; Greiner et al., 1994; Ellis et al., 1996). Besides, pions are much more stable than heavier particles which decay quickly, also, to pions.

The relative probability of production of keons and lambdas to that of pions ($R_{\pi/k} = \bar{n}_\pi/\bar{n}_k$ and $R_{\pi/\Lambda} = \bar{n}_\pi/\bar{n}_\Lambda$)

over the available energy range are displayed in Figure 4. $R_{\pi/\Lambda}$ shows remakable higher values than $R_{\pi/k}$ over all the available energy range, in agreement with Figure 3 and one may notice also that $R_{\pi/k}$ decreases with energy, while $R_{\pi/\Lambda}$ is almost constant. This might reflect that formation of different particles results from some changes of the nuclear matter state, which in turn, imposes different mechanisms for creating different particles e.g. the increased enhancement of gluon interactions around the TeV order of interaction energy (LHCb collaboration, 2012).

This study presented a general survey of qualitative descriptions of particle creation in the pp collision as a preliminary work for a next coming study that would go deeper in this open uncomplete subject, including more mathematical and computational details.
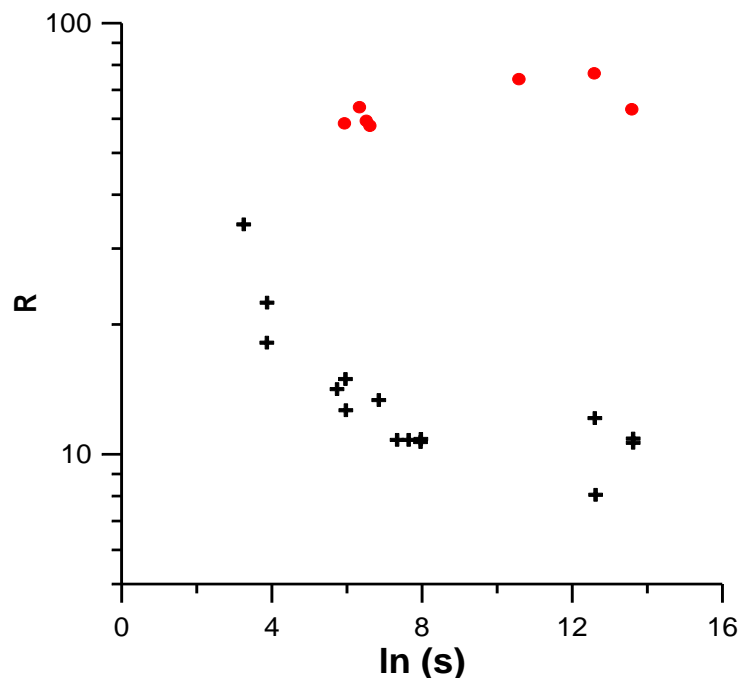
Figure 4. The dependence of the ratio, R, of mean multiplicities: pion to keon $R_{\pi/k}$ (black crosses), and pion to lambda $R_{\pi/\Lambda}$ (red blobs) on ln(s).

Conclusion

Along the studied energy range, the experimental data of created particles in proton proton interaction show different mechanisms that could be divided into three parts: soft, semi-hard and hard components. The soft component, which means that the final-state particles are created and emitted uncorrelated, seems to exist allover the considered range of energy. It is probably the only mechanism in particle creation up to several tens of GeVs. This nature changes as energy passes through several hundreds of GeVs region, where particles have the ability to emit additional particles by decay and cascade production, thus adding a semi-hard component to the soft one, in the creation process. This trend seems to indicate the existence of new phases in the interacting systems, presumably that the average number of created particles represents a macroscopic parameter eligible to probe the state of the system and its variation with interaction energy.

On approaching the borders of the TeV region, a hard component takes a leading role in creation in addition to the other components, as a result of the growth of the gluon interactions. Heavier particle production (like keons and lambdas) show remarkable lower production rate than pion. This might be due to the small bits of energy losses of the color field as excitation of soft gluons rather than by hard single gluon radiation. Beyond these limits, the results show that production of heavier particles than pions flourishes as the interaction energy grows up, where gluons jet, fragmentations and long reformations at enough energies furnish more suitable conditions for heavy quarks creation than quark jets do.

Conflict of Interest

The author(s) have not declared any conflict of interests.

REFERENCES

Adler SS, Afanasiev S, Aidala C, Ajitanand NN, Akiba Y, Alexander J, Amirikas R, Aphecetche L, Aronson SH, Averbeck R, Awes TC, Azmoun R, Babintsev V, Baldisseri A, Barish KN, Barnes PD, Bassalleck B, Bathe S, Batsouli S, Baublis V, Bazilevsky A, Belikov S, Berdnikov Y, Bhagavatula S, Boissevain JG, Borel H, Borenstein S, Brooks ML, Brown DS, Bruner N, Bucher D, Buesching H, Bumazhnov V, Bunce G, Burward-Hoy JM, Butsyk S, Camard X, Chai JS, Chand P, Chang WC, Chernichenko S, Chi CY, Chiba J, Chiu M, Choi IJ, Choi J, Choudhury RK, Chujo T, Cianciolo V, Cobigo Y, Cole BA, Constantin P, D'Enterria DG, David G, Delagrange H, Denisov A, Deshpande A, Desmond EJ, Dietzsch O, Drapier O, Drees A, Drees KA, Du Rietz R, Durum A, Dutta D, Efremenko YV, El Chenawi K, Enokizono A, En'yo H, Esumi S, Ewell L, Fields DE, Fleuret F, Fokin SL, Fox BD, Fraenkel Z, Frantz JE, Franz A, Frawley AD, Fung SY, Garpman S, Ghosh TK, Glenn A, Gogiberidze G, Gonin M, Gosset J, Goto Y, Granier De Cassagnac R, Grau N, Greene SV, Grosse Perdekamp M, Guryn W, Gustafsson HA, Hachiya T, Haggerty JS, Hamagaki H, Hansen AG, Hartouni EP, Harvey M, Hayano R, He X, Heffner M, Hemmick TK, Heuser JM, Hibino M, Hill JC, Holzmann W, Homma K, Hong B, Hoover A, Ichihara T, Ikonnikov VV, Imai K, Isenhower D, Ishihara M, Issah M, Isupov A, Jacak BV, Jang WY, Jeong Y, Jia J, Jinnouchi O, Johnson BM, Johnson SC, Joo KS, Jouan D, Kametani S, Kamihara N, Kang

JH, Kapoor SS, Katou K, Kelly S, Khachaturov B, Khanzadeev A, Kikuchi J, Kim DH, Kim DJ, Kim DW, Kim E, Kim GB, Kim HJ, Kistenev E, Kiyomichi A, Kiyoyama K, Klein-Boesing C, Kobayashi H, Kochenda L, Kochetkov V, Koehler D, Kohama T, Kopytine M, Kotchetkov D, Kozlov A, Kroon PJ, Kuberg CH, Kurita K, Kuroki Y, Kweon MJ, Kwon Y, Kyle GS, Lacey R, Ladygin V, Lajoie JG, Lebedev A, Leckey S, Lee DM, Lee S, Leitch MJ, Li XH, Lim H, Litvinenko A, Liu MX, Liu Y, Maguire CF, Makdisi YI, Malakhov A, Manko VI, Mao Y, Martinez G, Marx MD, Masui H, Matthias F, Matsumoto T, McGaughey PL, Melnikov E, Messer F, Miake Y, Milan J, Miller TE, Milov A, Mioduszewski S, Mischke RE, Mishra GC, Mitchell JT, Mohanty AK, Morrison DP, Moss JM, Mühlbacher F, Mukhopadhyay D, Muniruzzaman M, Murata J, Nagamiya S, Nagle JL, Nakamura T, Nandi BK, Nara M, Newby J, Nilsson P, Nyanin AS, Nystrand J, O'Brien E, Ogilvie CA, Ohnishi H, Ohja ID, Okada K, Ono M, Onuchin V, Oskarsson A, Otterlund I, Oyama K, Ozawa K, Pal D, Palounek AP, Pantuev VS, Papavassiliou V, Park J, Parmar A, Pate SF, Peitzmann T, Peng JC, Peresedov V, Pinkenburg C, Pisani RP, Plasil F, Purschke ML, Purwar AK, Rak J, Ravinovich I, Read KF, Reuter M, Reygers K, Riabov V, Riabov Y, Roche G, Romana A, Rosati M, Rosnet P, Ryu SS, Sadler ME, Saito N, Sakaguchi T, Sakai M, Sakai S, Samsonov V, Sanfratello L, Santo R, Sato HD, Sato S, Sawada S, Schutz Y, Semenov V, Seto R, Shaw MR, Shea TK, Shibata TA, Shigaki K, Shiina T, Silva CL, Silvermyr D, Sim KS, Singh CP, Singh V, Sivertz M, Soldatov A, Soltz RA, Sondheim WE, Sorensen SP, Sourikova IV, Staley F, Stankus PW, Stenlund E, Stepanov M, Ster A, Stoll SP, Sugitate T, Sullivan JP, Takagui EM, Taketani A, Tamai M, Tanaka KH, Tanaka Y, Tanida K, Tannenbaum MJ, Tarján P, Tepe JD, Thomas TL, Tojo J, Torii H, Towell RS, Tserruya I, Tsuruoka H, Tuli SK, Tydesjö H, Tyurin N, Van Hecke HW, Velkovska J, Velkovsky M, Villatte L, Vinogradov AA, Volkov MA, Vznuzdaev E, Wang XR, Watanabe Y, White SN, Wohn FK, Woody CL, Xie W, Yang Y, Yanovich A, Yokkaichi S, Young GR, Yushmanov IE, Zajc WA, Zhang C, Zhou S, Zolin L (PHENIX Collaboration) (2003). Midrapidity Neutral-Pion Production in Proton-Proton Collisions at √s=200 GeV. Phys. Rev. Lett. 91(24):241803.

Alexopoulos T, Anderson EW, Biswas NN, Bujak A, Carmony DD, Erwin AR, Gutay LJ, Hirsch AS, Hojvat C, Kenney VP, Lindsey CS, Losecco JM, Matinyan SG, Morgan N, Oh SH, Porile N, Scharenberg R, Stringfellow B, Thompson M, Turkot F, Walker WD, Wang CH (1998). The role of double parton collisions in soft hadron interactions. Phys. Lett. B435(3-4):453-457.

Ansorge RE, Åsman B, Burow L, Carlson P, DeWolf RS, Eckart B, Ekspong G, Fuglesang C, Gaudaen J, Geich-Gimbel C, Holl B, Hospes R, Jon-And K, Lotse F, Manthos N, Munday DJ, Ovens JEV, Pelzer W, Rushbrooke JG, Triantis F, Van Hamme L, Walck C, Ward CP, Ward DR, Webber CJS, White TO, Wilquet G, Yamdagni N (1989). Hyperon Production at 200 and 900 GeV c.m. Energy. Nucl. Phys. B328(1):36-58.

Anticic T, Baatar B, Bartke J, Betev L, Bialkowska H, Boimska B, Bracinik J, Cerny V, Chvala O, Dolejsi J, Eckardt V, Fischer HG, Fodor Z, Gladysz E, Kadija K, Karev A, Kolesnikov V, Kowalski M, Kreps M, Makariev M, Malakhov A, Mateev M, Melkumov G, Rybicki A, Schmitz N, Seyboth P, Susa T, Szymanski P, Trubnikov V, Varga D, Vesztergombi G, Wenig S (2010). Inclusive production of charged kaons in p+p collisions at 158 GeV/c beam momentum and a new evaluation of the energy dependence of kaon production up to collider energies. Eur. Phys. J. C68(1-2):1–73.

Antinucci M, Bertin A, Capiluppi P, D'agostino-Bruno M, Rossi AM, Vannini G, Giacomelli G, Bussière A (1973). Multiplicities of charged particles up to ISR energies. lettere El-Nuovo Cimento. 6(4):121-128.

Badawy BM (2008). Central collisions induced by light target nuclei. J. Nucl.Radiation Phys. 3(1):31-51.

Becattini F, Heinz U (1997). Thermal hadron production in pp and p$\bar{p}$ collisions. Zeitschrift für Physik C. Particles Fields. 76(2):269-286.

Samset BH (2006). Charged particle production in p+p collisions at √s = 200 GeV. Institute of Physics, University of Oslo, Ph.D thesis. pp. 36-37.

Biyajima M, Mizoguchi T, Nakajima T, Ohsawa NA, Suzuki N (2001). Analyses of multiplicity distributions at Tevatron by a two component stochastic model: No leading particle effect in E735 experiment. Phys. Lett. B515 (3-4):470-476.

Cerny V, Pisut J (1977). Charge transfer in multiparticle production and the behaviour of partons during the hadronic collision. Acta Physica Polonica. B8(6):469-473.

Collaboration CMC (Chatrchyan et al.) (2012). Shape, transverse size, and charged-hadron multiplicity of jets in pp collisions at s√=7TeV. JHEP. 2012(6):1-38.

LHCb Collaboration (Aaij R et al.) (2012). Measurement of the Ds+ - Ds- production asymmetry in 7 TeV pp collisions. Phys. lett. B713(3):186-195.

Ellis RK, Stirling WJ, Webber BR (1996). QCD and Collider Physics (the press syndicate of the University of Cambridge, United Kingdom) 1996, pp. 1-17.

Fiete J, Grosse O, Klaus R (2010). Charged-particle multiplicity in proton–proton collisions. J. Phys. G: Nucl. Part. Phys. 37(8):83001.

Giovannini A, van hove L (1986). Negative binomial multiplicity distributions in high energy hadron collisions. Z. Physik. C30(3):391-400.

Giovannini A, Ugoccioni R (1999). Possible scenarios for soft and semihard components structure in central hadron-hadron collisions in the TeV region: Pseudorapidity intervals. Phys. Rev. D60 (7):074027.

Greiner W, Horst S, André G (1994). Hot and Dense Nuclear Matter (Plenum press, New York) 1994, P. 23.

Gribov VN (1967). A Reggeon diagram technique. Sov. Phys. JETP 26:414.   http//pdg.lbl.gov/current/avg.multiplicity/. http://www.physics.adelaide.edu.au/~jbellido/cosmicraysschool/Charl as/RalphEngel/EngelLecture2.pdf

Hussein MT, Rabea A, El-Naghy A, Hassan NM (1995). A string model for hadron interaction at high energies. Progress Theor. Phys. 93(3):585-595.

Koba Z, Nielsen HB, Olsen P (1972). Scaling of multiplicity distributions in high energy hadron collisions. Nucl. Phys. B40:317-334.

Ashwini K, Singh BK, Srivastava PK, Singh CP (2013). Wounded Quarks and Multiplicity at Relativistic Ion Colliders. European Phys. J. Plus. 128(4):1-10.

Minami S (1973). Multiplicity distribution, two-component model of particle production and intercept of the Regge trajectory. Lettere Al Nuovo Cimento Series 2. 7(11):419-422.

Niccol`o M (1998). Faculty of mathematical, physical and natural sciences, university of Pavia, Italy. Ph.D thesis in Physics-XI cycle. pp. 21-30.

Regge T (1959). Introduction to complex orbital momenta. Nuovo Cimento. 14(5):951-976.

Engel R (2008). 3rd School on Cosmic Rays and Astrophysics, Arequipa, Perú. High Energy Cosmic Ray Interactions. pp. 15-16.

Rushbrooke JG (1982). A comparison of cosmic ray physics with latest accelerator data. J. Phys. Colloques. 43(C3):177-190.

STAR Collaboration (Adamczyk L et al.) (2014a). Energy Dependence of Moments of Net-Proton Multiplicity Distributions at RHIC. Phys. Rev. Lett. 112(3): 032302.

STAR Collaboration (Adamczyk L et al.) (2014b). Jet-Hadron Correlations in √s$_{NN}$ =200 GeV p+p and Central Au+Au Collisions. Phys. Rev. Lett. 112(12):122301.

Daniel S, Huston J, Pumplin J, Tung W-K (2003). Inclusive jet production, parton distributions, and the search for new physics. JHEP 10(46):1-35.

Tai A, Sa B-H (1998). Production of mini-(gluon) jets and strangeness enhancement in pA and AA collisions at relativistic energies. Phys. Rev. C57:261-265.

Tran T, Van J (1988). Current Issues in Hadron Physics: Proceedings of the XXIIIrd Rencontre De Moriond, Les Arcs, Savoie, France. pp. 3-18.

Walker WD (2004) Multiparton interactions and hadron structure. Phys. Rev. D. 69(3):034007.

Wolschin G (2011). Pseudorapidity distributions of produced charged hadrons in pp collisions at RHIC and LHC energies. EPL. 95(6):61001.

International Journal of Physical Sciences

Related Journals Published by Academic Journals

- ■African Journal of Pure and Applied Chemistry
- ■Journal of Internet and Information Systems
- ■Journal of Geology and Mining Research
- ■Journal of Oceanography and Marine Science
- ■Journal of Environmental Chemistry and Ecotoxicology
- ■Journal of Petroleum Technology and Alternative Fuels